Control of a Bidirectional Z-Source Inverter for Hybrid Electric Vehicles in Motoring, Regenerative Braking and Grid Interface Operations

Omar Ellabban, Joeri Van Mierlo and Philippe Lataire
Department of Electrical Engineering and Energy Technology
Vrije Universiteit Brussel
Pleinlaan 2, 1050 Brussels, Belgium
omar.ellabban@vub.ac.be

***Abstract*--This paper presents a battery supplying a bidirectional Z-Source Inverter (ZSI) feeding a three phase induction motor. The indirect field-oriented control (IFOC) method is used to control the induction motor speed during motoring and regenerative braking operations. The IFOC is implemented based on PWM voltage modulation with voltage decoupling compensation. A dual loop controller is designed, based on a small signal model, to control the bidirectional ZSI capacitor voltage using the bode diagram. In addition, this paper presents the gird interface mode with its control to charge or discharge the battery from the grid. MATLAB simulation results verified the validity of the proposed control strategies during motoring, regenerative braking and grid interface operations. Experimental setup of the bidirectional ZSI is under progress.**

***Index Terms*: Z-source Inverter, indirect field-oriented control, regenerative braking, grid interface.**

I. INTRODUCTION

With increasing oil price and global warming, automobile manufacturers are producing more hybrid electric vehicles (HEV) and electrical vehicles (EV). Many research efforts have been focused on developing efficient, reliable, and low-cost power conversion techniques for the future new energy vehicles. Hybrid Electric Vehicle use an electric energy source (battery or super capacitor) to assist the propulsion of the vehicle in addition to the primary energy source (internal combustion engine (ICE) or fuel cell (FC)), and to absorb the kinetic energy during regenerative braking. There are two basic configurations for power converters used in HEV: one is a traditional PWM inverter powered by a battery as shown in Fig.1, the other is an inverter plus a dc/dc converter as shown in Fig.2. Usually a bidirectional dc/dc converter is used, it acts as a boost converter during motoring operation to drive the traction motor for a high speed and a high torque and it works as a buck converter to capture the regenerative braking energy. So the bidirectional power transfer is of course desirable and leads to improve the HEV's efficiency for transient drive cycles. The battery voltage variation in HEVs could be as large as 50% and depends on the battery type. With this voltage range, the traditional PWM inverter has to be oversized to handle the full voltage and twice the current at 50% of the battery voltage to output the full power, which increases the cost of the inverter. The dc/dc boosted PWM inverter can minimize the stress of the inverter with an extra bidirectional dc/dc stage; however, this increases the system cost, complexity, and reduces the reliability [1].

The Z-Source Inverter (ZSI), shown in Fig. 3, is a single-stage dc/ac power converter that can perform both inversion and voltage buck/boost without using two separate power converters [2]. Due to the less number of power converters, it reduces the power losses, size, cost and complexity compared to its two converters counterpart. Special Z-network of two capacitors and two inductors connected to the well known three phase bridge, allows working in buck or boost mode using the shoot-through state. There are three different topologies for the three phase two level ZSI as voltage source, they are: the basic ZSI, the bidirectional ZSI and the high performance ZSI [3]. The basic version of ZSI can be changed into a bidirectional ZSI by replacement of the input diode D by a bidirectional switch S_7, as shown in Fig. 4. The bidirectional ZSI is able to exchange energy between ac and dc energy storage in both directions. Also, the bidirectional ZSI is able to completely avoid the undesirable operation modes when the ZSI operated under a small inductance or low load power factor [4-7]. All PWM control method can be applied for the bidirectional ZSI after determining the drive signal of S_7. From the analysis of different operation models of the bidirectional ZSI presented in [8], the switch S_7 has to operate in off state during the inverter operated in the shoot-through state, so the drive signal of the S_7 is complement with the shoot-through signal. The closed loop control of the Z-network capacitor voltage of a basic ZSI and the peak dc-link voltage of a high performance ZSI are presented in [9, 10]. A grid interface mode as proposed in [4, 11] enables the bidirectional ZSI to exchange energy between the grid and the dc energy in both directions.

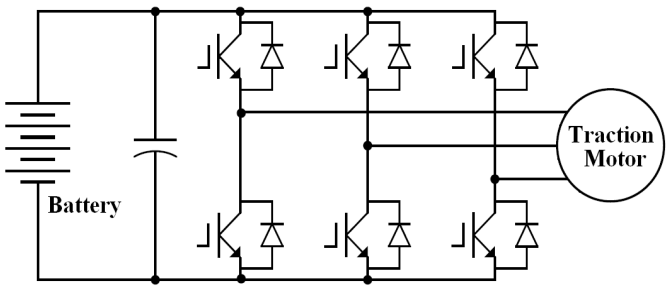

Fig. 1 Traditional PWM inverter for HEV applications

2010 IEEE Electrical Power & Energy Conference
978-1-4244-8188-0/10/$26.00 ©2010 IEEE

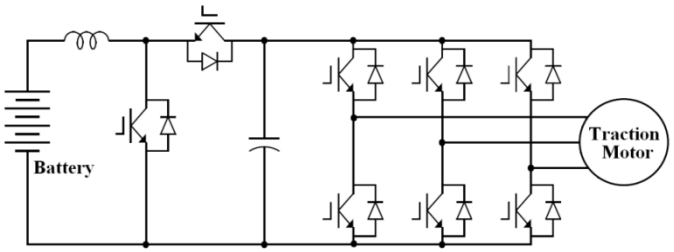

Fig. 2 DC/DC boosted PWM inverter for HEV applications

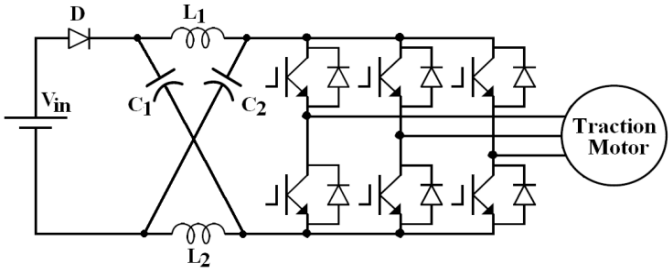

Fig. 3 Basic Z-source inverter

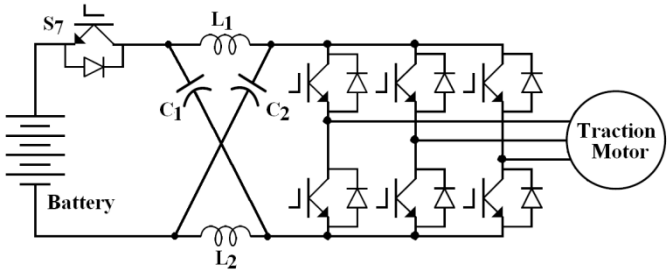

Fig. 4 Bidirectional Z-Source inverter for HEV applications

The major types of electric traction motors adopted for HEVs include the dc motor, the induction motor (IM), the permanent magnet synchronous motor (PMSM), and the switched reluctance motor (SRM). According to the comparative study presented in [12], the IM seems to be the most adapted candidate for the electric propulsion of HEVs. In order to control the speed and the torque of an induction motor, the indirect field-oriented control (IFOC) is used [13].

II. Operations Modes And Modeling Of Bidirectional ZSI

From the point of view of energy storage, the basic topology of the Z-source inverter is useless, due to possible energy transfer only from dc to ac side. The only way to change the basic version of the Z-source inverter into a bidirectional system is the replacement of the input diode D by a bidirectional switch S_7. Additional switch S_7 is thought to operate during the regenerative mode in the same manner as the diode during the inverter mode and its gate signal is a logical function of the main bridge switches. The bidirectional ZSI operates in different seven operation modes from the relationships, as shown in Fig. 5 [8]. A third order model of current relationships, but these seven operation modes are generalized as two basic modes in view of the voltage

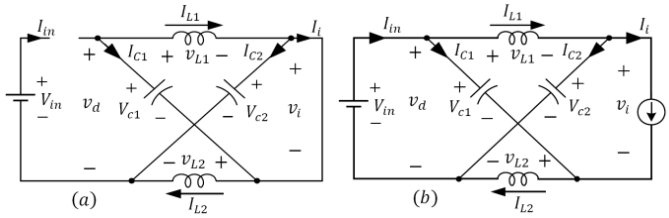

Fig. 5 The basic two equivalent operation modes: (a) shoot-through state, (b) non shoot-through state

the bidirectional ZSI can be illustrated by simplifying the ac side circuit to an equivalent dc load $Z_l = R_l + j\omega L_l$, where, R_l is calculated by power balance as $R_l = 8|Z_l|/3\cos\phi$ and L_l is determined so that the time constant of the dc load is the same as the ac load. The state variables are: capacitor voltage v_c, inductor current i_L, and load current i_l. The shoot-through duty ratio to capacitor voltage $G_{vd}(s)$ and shoot-through duty ratio to inductor current $G_{id}(s)$ small signal transfer functions of the bidirectional ZSI with inductive load are given by Eqs. 1,2 at the bottom of this page [10], where $V_{in}, R_l, L_l, I_L, V_C, I_l, D_0$ are input battery voltage, equivalent dc load resistance, equivalent dc load inductance, and steady state values of inductor current, capacitor voltage, load current and shoot-through duty ratio at certain operating point respectively, and L, C are the Z-network capacitor and inductor.

III. Capacitor Voltage Control

The capacitor voltage control is implemented using a dual loop control strategy using Eqs. (1, 2) as shown in Fig. 6. The loop gains for inner current loop $T_i(s)$ and outer voltage loop $T_v(s)$ can be expressed as

$$T_i(s) = G_{ci}(s)G_M(s)G_{id}(s)$$
$$T_v(s) = \frac{G_{cv}(s)G_M(s)G_{vpd}(s)}{1+T_i(s)} \quad (3)$$

where $G_{cv}(s)$, $G_{ci}(s)$ and $G_M(s)$ are the outer voltage loop controller, the inner current loop controller and the modified modulation transfer function, respectively.

For outer voltage and inner current loops, a two poles and one zero controller has been designed to compensate the low-frequency loop gain and improving the phase margin, whose transfer function is

$$G_c(s) = G_{c0}\frac{\left(1+\frac{s}{\omega_z}\right)}{s\left(1+\frac{s}{\omega_p}\right)} \quad (4)$$

To design this controller: first, the new crossover frequency f_c is chosen; then, choose an arbitrary value for the phase margin; then, the pole and zero frequencies are chosen as;

$$f_z = f_c\sqrt{\frac{1-\sin(\theta)}{1+\sin(\theta)}}, f_p = f_c\sqrt{\frac{1+\sin(\theta)}{1-\sin(\theta)}} \quad (5)$$

finally, the controller gain G_{c0} is

$$G_{c0} = \left|\frac{1}{T(s)}\right|_{f=f_c} \quad (6)$$

$$G_{vd}(s) = \frac{(-2I_L+I_l)L_lLs^2+[(-2I_L+I_l)R_lL+(1-D_0)(2V_C-V_{in})L+(1-2D_0)(2V_C-V_{in})L_l]s+(1-2D_0)(2V_C-V_{in})R_l}{L_lLCs^3+R_lLCs^2+[2L(1-D_0)^2+L_l(2D_0-1)^2]s+R_l(2D_0-1)^2} \quad (1)$$

$$G_{id}(s) = \frac{(2V_C-V_{in})L_lCs^2+[R_lC(2V_C-V_{in})+(1-2D_0)(-2I_L+I_l)L_l]s+(1-D_0)(2V_C-V_{in})+(1-2D_0)(-2I_L+I_l)R_l}{L_lLCs^3+R_lLCs^2+[2L(1-D_0)^2+L_l(2D_0-1)^2]s+R_l(2D_0-1)^2} \quad (2)$$

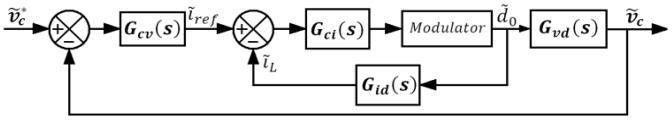

Fig. 6 Dual loop capacitor voltage control block diagram of a bidirectional ZSI

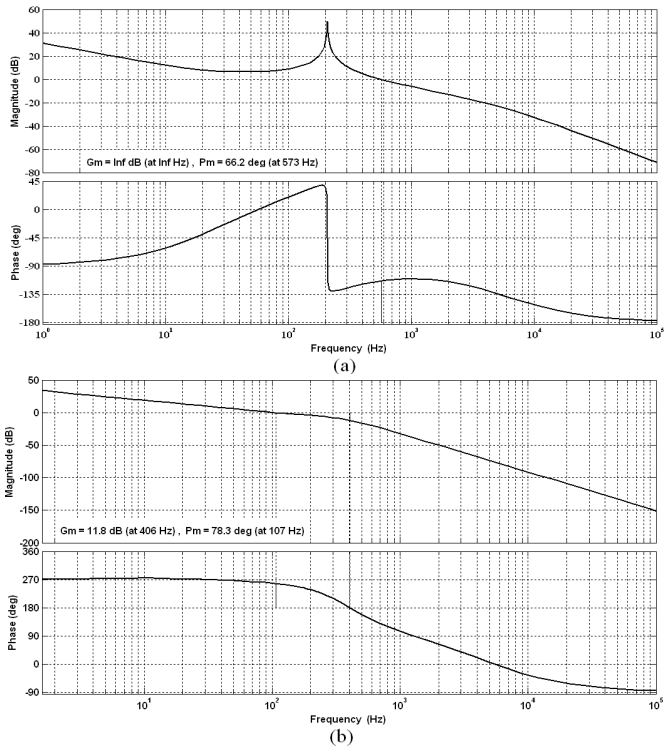

Fig. 7 Frequency response of current and voltage loop gains

Figure 7 show the bode plots for the current loop gain and voltage loop gain, respectively, using the parameters in Table I in the appendix. The plots indicate that the current loop gain has a crossover frequency as 570 Hz, with a phase margin of 66°,as shown in Fig. 7-a. To avoid interaction between the sub-systems, low control bandwidth is used for voltage loop. The resulting outer voltage loop has a crossover frequency of 107 Hz and a phase margin of 78°, as shown in Fig. 7-b.

IV. Motoring And Regenerative Operation Modes Control

In order to achieve high dynamic performance in an induction motor drive application during motoring and regenerative braking operations, the vector control is often applied. The indirect field oriented controlled (IFOC) IM drive is widely used in high performance applications due to its simplicity and fast dynamic response. The indirect field-oriented control based on PWM voltage modulation with voltage decoupling compensation is used to insert the shoot-through state within the switching signals, as shown in Fig. 8. The parameters of the four PI controllers are calculated based on the desired damping and dynamics response [13].

Figure 9 shows the entire closed loop system containing: the input battery, the bidirectional ZSI, the capacitor voltage controllers and the IFOC speed controller, where the capacitor

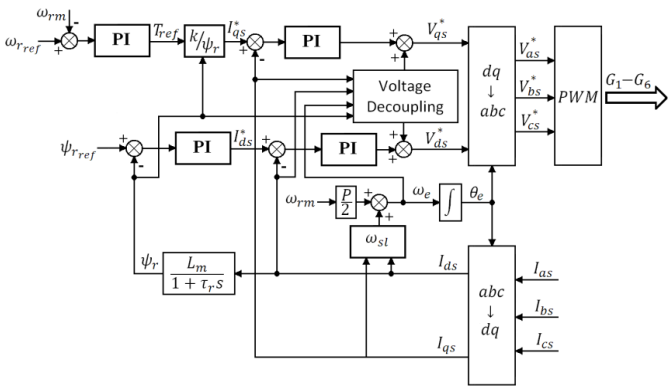

Fig. 8 Block diagram of the IFOC of induction motor

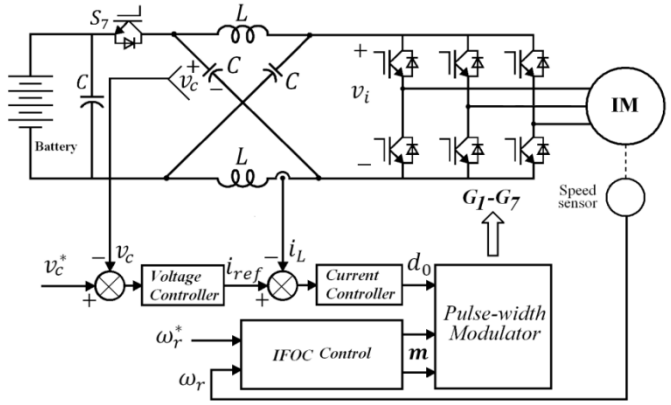

Fig. 9 Closed loop speed control of three phase induction motor fed by a bidirectional ZSI

voltage control generates the shoot-through duty ratio and the IFOC generates the modulation index according to an operating condition.

V. Grid Charging/Discharging Operation Mode Control

The main goal of the control system where the bidirectional ZSI is used to interface between the three phase grid and the battery is to exchange the required power between both, either to charge the battery or to supply power to the grid. By using the DC controller to regulate the capacitor voltage and hence the dc-link voltage at a certain level, the Z-source inverter can be conveniently regulated by a current control method. Thus, an effective algorithm of AC currents control is needed. The controllers for the AC side of the inverter were designed in the stationary reference frame using a proportional plus a resonance controller (PR), its transfer function is [11]

$$G_c(s) = K_p + \frac{2K_i s}{s^2+\omega_0^2} \quad (7)$$

where K_p, K_i and ω_0 are the proportional gain, the integral gain and the angular frequency at fundamental grid frequency. The resonance controller gives infinite gain at the fundamental frequency that would result in integral action in that particular frequency while removing the steady state error. Fig. 10 shows the control strategy of a grid connected bidirectional ZSI. Where P^* the required is power injected to or drawn from the three phase grid, using this power and the measured grid

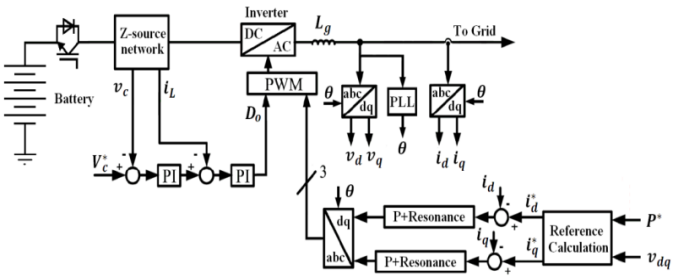

Fig. 10 Control strategy of grid connected bidirectional ZSI

voltage components in the stationary reference frame v_d, v_q, the reference currents are calculated by,

$$i_d^* = \frac{v_d}{v_d^2+v_q^2} \cdot P^* \qquad (8)$$
$$i_q^* = \frac{v_q}{v_d^2+v_q^2} \cdot P^*$$

The phase angle θ of the grid voltage is detected by a phase-locked loop (PLL) and is used in the abc-dq and dq-abc transformations. The two PR controllers are used to control the d and q axis output current components respectively. The output of these controllers is transformed from dq to abc to generate the modulation signals, as shown in Fig. 10.

VI. Simulation Results

In order to verify the proposed control strategies during motoring, regenerative braking and grid connection, two simulation models are carried out using MATLAB/ SIMULINK software. The first model is used to verify the proposed control strategy during the motoring and the regenerative braking operation modes of a 15 kw induction motor. The second model is used to verify the proposed control strategy during grid charging/discharging operation mode with active power up to 15 kW. The parameters of both models are presented in the appendix. Figs. 11-14 show the bidirectional ZSI feeding an induction motor response during motoring and regenerative braking operation modes. The system is operated in different operation modes, as shown in Fig. 11: acceleration mode with the rated torque during the time interval: 0-0.2 sec, steady state operation mode with the rated torque and the rated speed during the time interval: 0.2-0.6 sec, overloaded transient mode with 1.2 of the rated torque and the rated speed during the time interval: 0.6-1 sec, deceleration transient mode from the rated speed to half the rated speed with the rated torque during time interval: 1-1.2 sec, light load transient mode with half the rated load and half the rated speed during the time interval: 1.2-1.6 sec, regenerative braking mode with the rated load during the time interval: 1.6-1.8 sec and standstill mode during the time interval 1.8-1.9 sec. Fig. 12 shows the following: the reference and the actual values of the Z-network capacitor voltage, where the capacitor voltage is controlled to be 653 V; the dc link voltage, which is changing, even while the capacitor voltage being controlled; the shoot-through duty ratio which is generated from the capacitor voltage control; the modulating signals which is generated from the IFOC control and the reference and actual Z-network inductor currents.

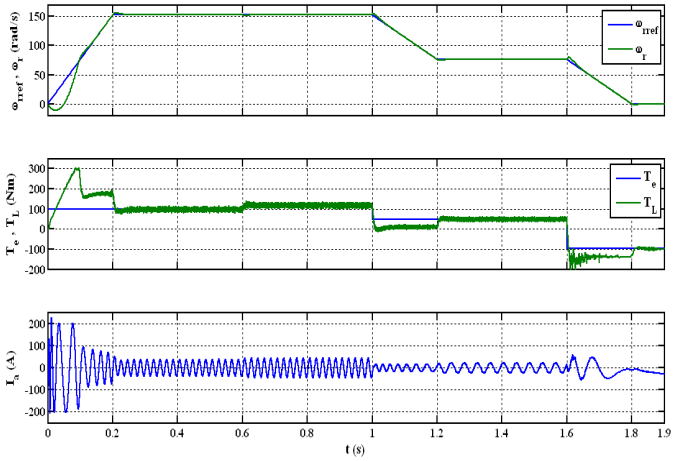

Fig. 11 Motor response during motoring and regenerative braking operation modes

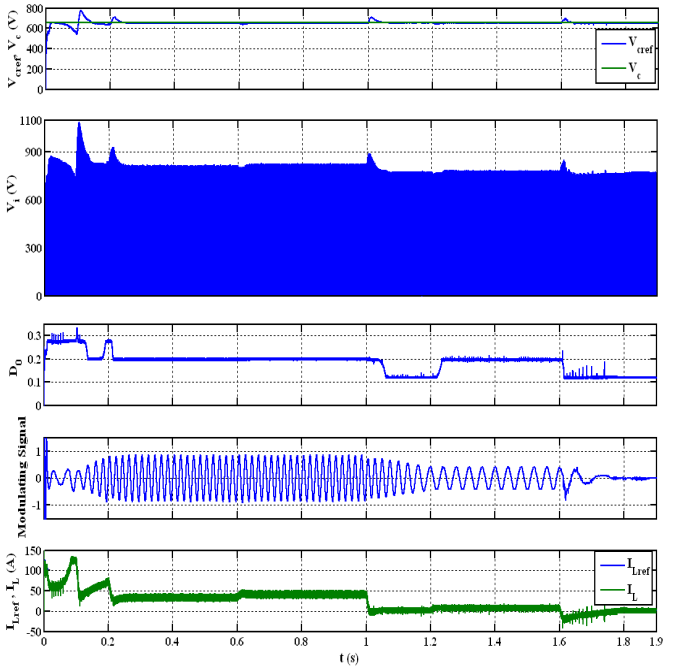

Fig. 12 bidirectional ZSI response during motoring and regenerative braking operation modes

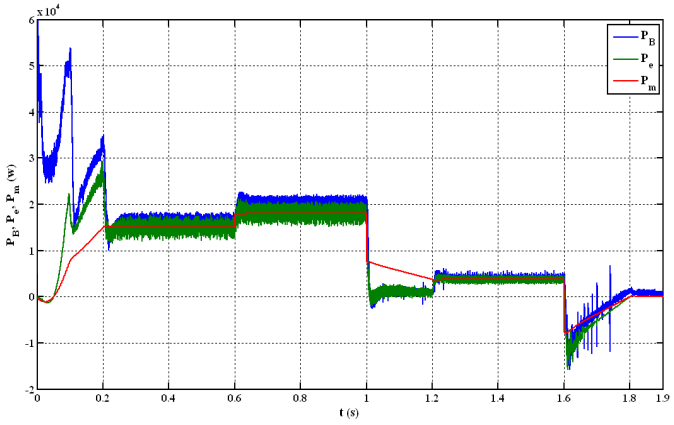

Fig. 13 Battery power and motor electric and mechanical powers during motoring and regenerative braking operation modes

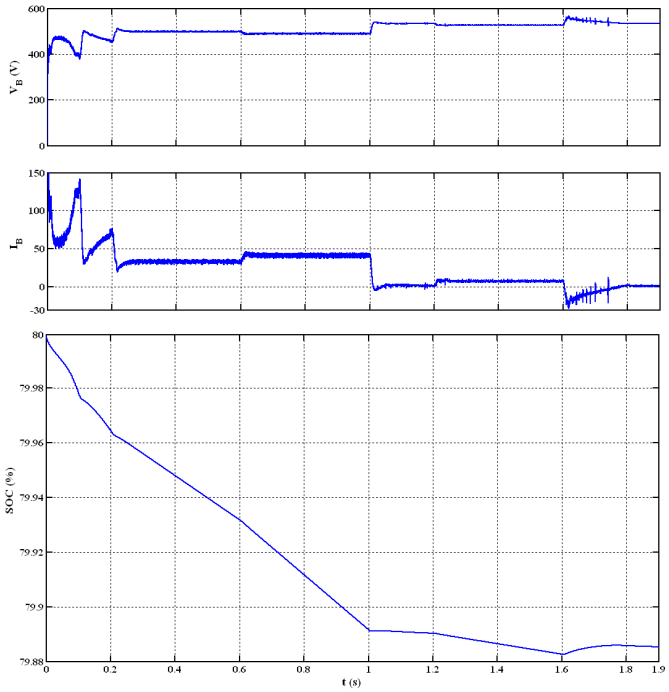

Fig. 14 Battery voltage, current and state of charge (SOC) during motoring and regenerative braking operation modes

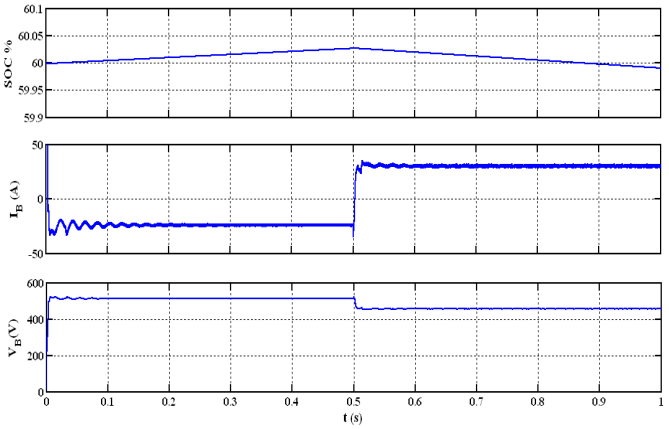

Fig. 15 Battery state of charge (SOC), voltage and current and during grid charging/discharging operation mode

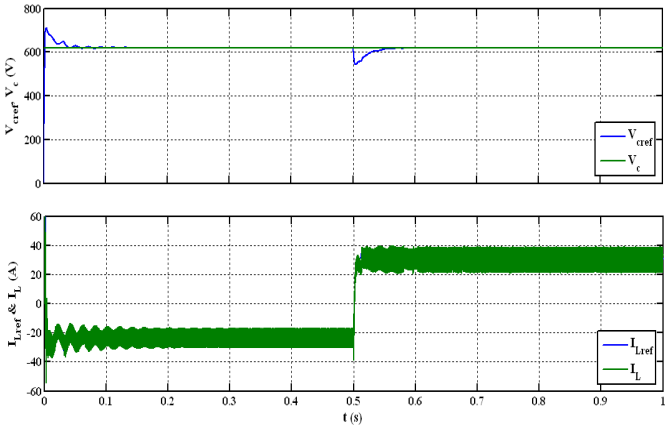

Fig. 16 Z-network capacitor voltage and inductor current and during grid charging/discharging operation mode

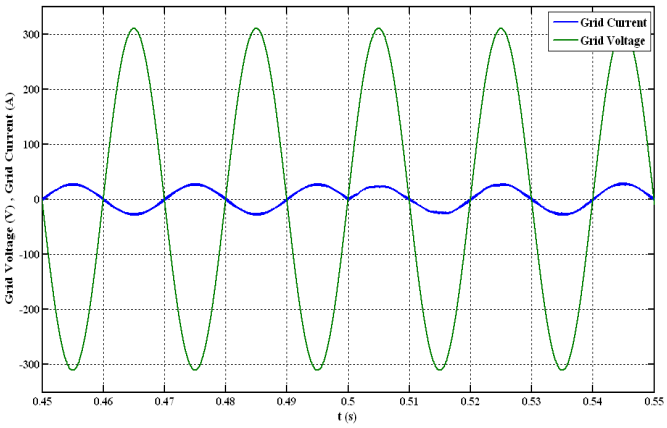

Fig. 17 Grid voltage and current during transition between charging/discharging operation modes

Fig. 13 shows the battery power and motor's electric and mechanical powers. Fig. 14 shows the battery voltage, current and the state of charge (SOC) and their change during the above mentioned operations modes. Figs. 15-17 show the grid connected bidirectional ZSI during charging and discharging operation mode modes. The simulation mode is operated for one sec in two different operation modes: battery charging from the grid during the time interval: 0-0.5 sec and battery discharging to the grid during the time interval: 0.5-1 sec. Fig. 15 shows the battery SOC, current and voltage, where the SOC increases during battery charging (negative battery current) and decreases during battery discharging (positive battery current). Fig. 16 shows the Z-network capacitor voltage and inductor current during battery charging and discharging. Fig. 17 shows the grid voltage and current during the transition between charging and discharging operation modes at t=0.5sec.

VII. FUTURE RESEARCH WORK

In order to verify the obtained simulation results, an experimental setup of a 30 kW bidirectional ZSI is designed and constructed in our laboratory to derive a 19 kW induction motor and it is now in testing mode.

VIII. CONCLUSIONS

This paper presents two control strategies of a bidirectional Z-source inverter. The first control strategy utilizes the indirect field-oriented control (IFOC) method to control the induction motor speed during motoring and regenerative braking operation modes. The second control strategy utilizes the proportional plus resonance (PR) controller to control the AC current for connecting the bidirectional ZSI to the grid. In both control strategies the Z-network capacitor voltage is controlled by a dual loop control. The first control strategy is tested during standard (acceleration, steady state, regenerative braking and standstill) and transient (overload, deceleration and light load) modes. The second control strategy is tested during battery charging from and discharging to the three phase grid. MATLAB simulation results verified the validity of the both control strategies during motoring, regenerative braking and grid interface operations.

Appendix

Table I System Parameters

Parameter	Value
Bidirectional ZSI parameters	
Inductance	500 μH
Capacitance	500 μF
Switching frequency	10 kHz
Battery package parameters	
Rated capacity	11 Ah
Nominal voltage	490 V
Internal resistance	1.11 Ω
Induction Motor Parameters	
Output power	15 kW
RMS line voltage	400 V
Input frequency	50 Hz
No. of poles	4
Stator resistance, R_s	0.2205 Ω
Rotor resistance, $\acute{R}_r$	0.2147 Ω
Stator inductance, L_{ls}	0.991 mH
Rotor inductance, $\acute{L}_{lr}$	0.991 mH
Mutual inductance, L_m	64.19 mH
Inertia, J	0.102 kg. m2
Fraction factor, F	0.009541 N.m.s
Grid Parameters	
Nominal grid voltage	380 V(RMS- LL)
Grid inductance	5 mH

REFERENCES

[1] Miaosen Shen and Fang Zheng Peng, "Converter systems for hybrid electric vehicles", International Conference on Electrical Machines and Systems 2007, pp. 2004 - 2010

[2] F. Z. Peng, "Z-source inverter", IEEE Transactions on Industry Applications, Vol. 39, no. 2, pp. 504-510.

[3] Omar Ellabban, Joeri Van Mierlo and Philippe Lataire, "Comparison between Different PWM Control Methods for Different Z-Source Inverter Topologies", the 13th European Conference on Power Electronics and Applications, EPE '09. 8-10 Sept. 2009, Barcelona-Spain.

[4] J. Rabkowski, "The bidirectional Z-source inverter as an energy storage/grid interface", EUROCON 2007, Sept. 2007, pp. 1629 – 1635.

[5] J. Rabkowski, "The bidirectional Z-source inverter for energy storage application", 2007 European Conference on Power Electronics and Applications, Sept. 2007, pp. 1-10.

[6] J. Rabkowski, R. Barlik, and M. Nowak, "Pulse Width Modulation methods for bidirectional/high-performance Z-source inverter", IEEE Power Electronics Specialists Conference, June 2008, pp. 2750 – 2756.

[7] Sumedha Rajakaruna and Bowen Zhang, "Design and Control of a Bidirectional Z-Source Inverter", Australasian Universities Power Engineering Conference, AUPEC 2009, 27-30 Sept. 2009, pp 1-6.

[8] Haiping Xu; Peng, F.Z.; Lihua Chen; Xuhui Wen, "Analysis and design of Bi-directional Z-source inverter for electrical vehicles", the Twenty-Third Annual IEEE Applied Power Electronics Conference and Exposition, APEC 2008, 24-28 Feb, pp:1252 – 1257.

[9] Ding, Xinping Qian, Zhaoming Yang, Shuitao Cui, Bin Peng, Fangzheng, "A PID Control Strategy for DC-link Boost Voltage in Z-source Inverter", the Twenty Second Annual IEEE Applied Power Electronics Conference, APEC 2007, pp. 1145-1148.

[10] Omar Ellabban, Joeri Van Mierlo and Philippe Lataire, "Voltage Mode and Current Mode Control for a 30 kW High-Performance Z-Source Inverter", IEEE Electrical Power & Energy Conference (EPEC), 22-23 Oct. 2009, Montreal, Canada.

[11] D. Mahinda Vilathgamuwa, Wang Xiaoyu, C. J. Gajanayake, "Z-source Converter Based Grid-interface For Variable-speed Permanent Magnet Wind Turbine Generators", IEEE Power Electronics Specialists Conference, PESC 2008, 15-19 June, pp:4545–4550.

[12] M. Zeraoulia, M. E. H. Benbouzid, D Diallo, "Electric motor drive selection issues for HEV propulsion systems: a comparative study," IEEE Transactions on Vehicular Technology, vol. 55, no. 6, Nov. 2006, pp.1756-1764.

[13] Chunting Mi, "Field-oriented Control of Induction Motor Drives with Direct Rotor Current Estimation for Application in Electric and Hybrid Vehicles", Journal of Asian Electric Vehicle, vol. 5, no. 2, pp. 1 - 4, December 2007.